Favored noncollective oblate states in light tellurium isotopes

E. S. Paul
Oliver Lodge Laboratory, University of Liverpool, P.O. Box 147, Liverpool L69 3BX, United Kingdom

D. B. Fossan, J. M. Sears, and I. Thorslund
Department of Physics, State University of New York at Stony Brook, Stony Brook, New York 11794
(Received 28 June 1995)

We have used cranking calculations, based on the total Routhian surface formalism, to investigate the medium spin structure ($I<25\hbar$) of light tellurium isotopes with $A\leqslant 122$. Several energetically favored non-collective oblate ($\gamma=+60°$) states, based on the aligned $\pi[(g_{7/2})^2]_{6^+}\otimes\nu[(d_{5/2})^x(h_{11/2})^y]$ configuration ($x=0,1$, $y=1-4$), are found to coexist with weakly deformed collective structures. Particularly favored 16^+ states are predicted for the even Te isotopes, while $39/2^-$ states are predicted for the odd Te isotopes. The theoretical results are compared to available experimental data.

PACS number(s): 21.10.Re, 27.60.+j, 23.20.Lv

Nuclei with proton and neutron numbers near shell closures are particularly rich in nuclear structure. The small yet finite number of valence particles (holes) is able to break the spherical symmetry and induce, albeit small, nuclear deformation. Because the small (prolate) deformation requires high angular velocity to generate collective angular momentum, specific noncollective "aligned" oblate states, where the nuclear spin is made up completely from single-particle angular momentum contributions, are able to compete energetically with the weakly deformed collective structures.

In the region of the nuclear chart just above the $Z=50$ shell closure with $N\approx 64$, energetically favored (yrast) oblate states were originally predicted at spin $I\approx 35\hbar$ in the light barium ($Z=56$) isotopes [1]; however, to date no experimental evidence has been found for such states. Subsequently, calculations based on a deformed Woods-Saxon single-particle potential [2,3] indicated similar oblate states at $I=(20-30)\hbar$ in xenon ($Z=54$) isotopes [4]. Indeed, evidence for such noncollective oblate states has been presented for several Xe isotopes with $A\approx 120$ [5–8]. Furthermore, similar yrast oblate states at $I^\pi=39/2^-$ and $43/2^-$ have been found in the series of odd-A iodine ($Z=53$) isotopes ranging from ^{115}I up to ^{121}I [9–12]. Recent investigations of odd-A tellurium ($Z=52$) isotopes have also identified unusually low-lying $39/2^-$ states, which have again been interpreted in terms of aligned noncollective oblate configurations [13,14]. These new experimental results have prompted us to perform cranking calculations, based on the total Routhian surface (TRS) formalism [15–17], for light tellurium isotopes ($A\leqslant 122$), in order to investigate further the influence of aligned noncollective oblate configurations along the yrast line. The theoretical predictions are compared to available experimental data.

For the light Te isotopes, the proton Fermi surface lies among the first members of $\pi g_{7/2}$ and $\pi d_{5/2}$ orbitals with $\Omega=1/2$, where Ω is the projection of the single-particle angular momentum onto the nuclear symmetry axis, for prolate shapes, and $\Omega=7/2$, 5/2 for oblate shapes. The unique-parity

TABLE I. TRS calculated noncollective oblate states in light tellurium isotopes ($A\leqslant 122$). The predicted quadrupole deformation for these states is $\beta_2\sim 0.15$. Particularly favored states are labeled with an asterisk. Only these favored states are listed for the odd-A isotopes.

(Parity, Signature)	I^π		Aligned configuration
(+,0)	6^+		$\pi[(g_{7/2})^2]_{6^+}$
(−,0)	8^-		$\pi[(d_{5/2})(h_{11/2})]_{8^-}$
(−,1)	9^-		$\pi[(g_{7/2})(h_{11/2})]_{9^-}$
(−,0)	14^-	*	$\pi[(g_{7/2})^2]_{6^+}\otimes\nu[(d_{5/2})(h_{11/2})]_{8^-}$
(+,0)	16^+	*	$\pi[(g_{7/2})^2]_{6^+}\otimes\nu[(h_{11/2})^2]_{10^+}$
(+,0)	16^+		$\pi[(d_{5/2})(h_{11/2})]_{8^-}\otimes\nu[(d_{5/2})(h_{11/2})]_{8^-}$
(+,1)	17^+		$\pi[(g_{7/2})(h_{11/2})]_{9^-}\otimes\nu[(d_{5/2})(h_{11/2})]_{8^-}$
(−,0)	18^-		$\pi[(d_{5/2})(h_{11/2})]_{8^-}\otimes\nu[(h_{11/2})^2]_{10^+}$
(−,1)	19^-	*	$\pi[(g_{7/2})(h_{11/2})]_{9^-}\otimes\nu[(h_{11/2})^2]_{10^+}$
(+,0)	22^+		$\pi[(g_{7/2})^2]_{6^+}\otimes\nu[(h_{11/2})^4]_{16^+}$
(−,0)	22^-	*	$\pi[(g_{7/2})^2]_{6^+}\otimes\nu[(d_{5/2})(h_{11/2})^3]_{16^-}$
(−,± 1/2)	$21/2^-$,$23/2^-$	*	$\pi[(g_{7/2})^2]_{6^+}\otimes\nu[(h_{11/2})]_{9/2^-,11/2^-}$
(−,± 1/2)	$37/2^-$,$39/2^-$	*	$\pi[(g_{7/2})^2]_{6^+}\otimes\nu[(h_{11/2})^3]_{25/2^-,27/2^-}$
(+,+1/2)	$37/2^+$	*	$\pi[(g_{7/2})^2]_{6^+}\otimes\nu[(d_{5/2})(h_{11/2})^2]_{25/2^+}$

0556-2813/95/52(6)/2984(5)/$06.00

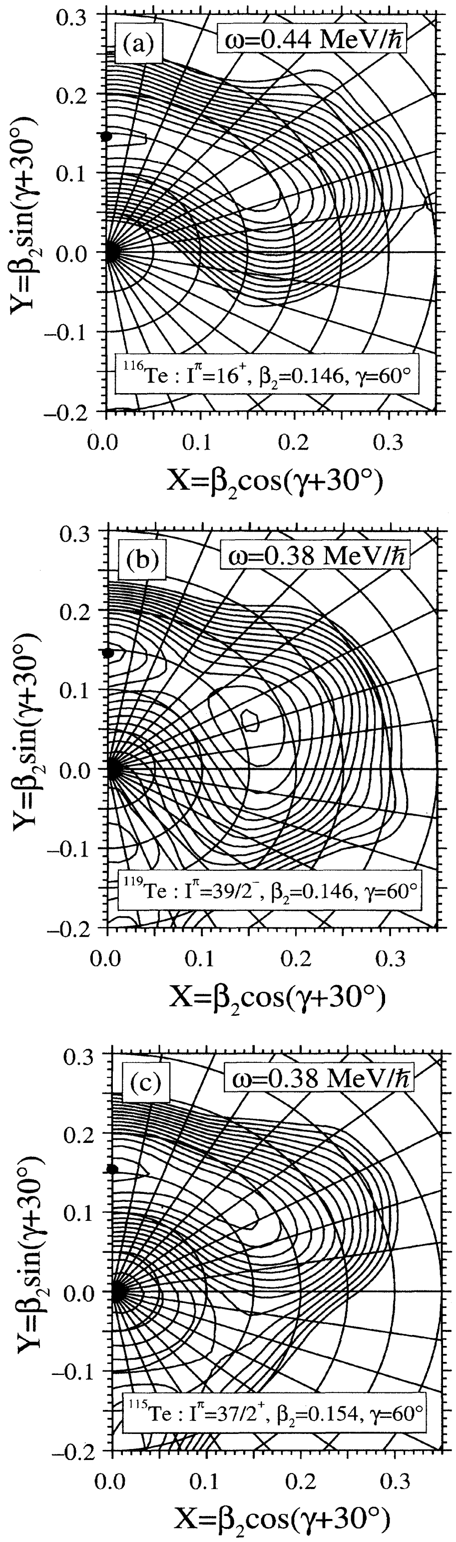

FIG. 1. Examples of TRS predicted aligned noncollective oblate states at $I^{\pi}=16^{+}$ in ^{116}Te (a), $I^{\pi}=39/2^{-}$ in ^{119}Te (b), and $I^{\pi}=37/2^{+}$ in ^{115}Te (c). The surfaces are calculated at constant frequency and the spin and deformation parameters of the oblate energy minimum indicated. The energy contours are separated by 140 keV.

$\pi h_{11/2}$ orbital lies just above the Fermi surface. For the range of neutron numbers under consideration ($N\approx 64$), the neutron Fermi surface lies near low-Ω $\nu g_{7/2}$, $\nu d_{5/2}$, and $\nu h_{11/2}$ orbitals for prolate shapes, and near high-Ω $\nu g_{7/2}$, $\nu d_{5/2}$, and $\nu h_{11/2}$ orbitals for oblate shapes. Thus, for oblate shapes where the nuclear symmetry and "rotation" axes coincide, a significant amount of single-particle angular momentum is available to generate the nuclear spin, and such noncollective configurations can compete energetically with the collective structures.

Deformation self-consistent cranking calculations, based on the TRS formalism [15–17], have been performed for quasiparticle configurations in Te isotopes with specific values of parity and signature: $(\pi,\alpha)=(\pi,\alpha)_{\rm protons}\otimes(\pi,\alpha)_{\rm neutrons}$. These calculations are based on a universal Woods-Saxon single-particle potential [2,3] and a monopole pairing residual interaction, where the pairing gaps have been calculated at zero frequency and allowed to decrease with increasing rotational frequency (e.g., see Ref. [16]). Generally, weakly deformed collective shapes are predicted at low spin in the Te isotopes with deformation parameters $\beta_2\approx 0.15$, $\gamma\approx 0°$. In addition, several noncollective oblate states ($\beta_2\approx 0.15$, $\gamma=+60°$) are found, some of which are predicted to be yrast for particular (π,α) configurations. These oblate states are summarized in Table I, while examples of the favored states for specific nuclei are shown in Fig. 1. Finally, a further set of noncollective oblate states shows up in the calculations, with a large quadrupole deformation $\beta_2\approx 0.30$. These well-deformed oblate states are, however, found to be well above yrast in excitation energy.

For even Te isotopes, a favored oblate state is predicted at $I^{\pi}=16^{+}$ based on the fully aligned $\pi[(g_{7/2})^2]_{6^+}\otimes\nu[(h_{11/2})^2]_{10^+}$ configuration, and this state is shown in Fig. 1(a) for ^{116}Te. Experimentally, low-lying 16^{+} states have been observed in ^{114}Te [18], ^{116}Te [19], ^{118}Te [20], and ^{120}Te [21], which we identify with this oblate state. A corresponding state is not observed in lighter even Te isotopes [22,23] since the oblate neutron Fermi surface is falling below the $\nu h_{11/2}$ shell making such a state energetically expensive. In Fig. 2, we show experimental rigid-rotor plots for the even $^{114-120}$Te isotopes, where a rotating liquid-drop energy reference, equal to $(\hbar^2/2\mathscr{J}_{\rm rig})I(I+1)$ MeV, has been subtracted. The rigid-body moment of inertia, $\mathscr{J}_{\rm rig}$, has been normalized to ^{158}Er [24], such that $(\hbar^2/2\mathscr{J}_{\rm rig})=0.007(158/A)^{5/3}$ MeV, where A is the mass number. A low-lying negative-parity $I^{\pi}=14^{-}$ noncollective oblate state is also predicted, based on the aligned $\pi[(g_{7/2})^2]_{6^+}\otimes\nu[(d_{5/2})(h_{11/2})]_{8^-}$ configuration. Low-lying 14^{-} states are indeed seen in ^{114}Te [18] and ^{116}Te [19], as shown in Figs. 2(a) and 2(b), which we may associate with the predicted oblate state. A similarly low-lying 14^{-} state is also observed in the lighter ^{112}Te isotope [22].

At higher spin, energetically favored oblate states are predicted at $I^{\pi}=22^{+}$ and 22^{-}, based on the aligned $\pi[(g_{7/2})^2]_{6^+}\otimes\nu[(h_{11/2})^4]_{16^+}$ and $\pi[(g_{7/2})^2]_{6^+}\otimes\nu[(d_{5/2})(h_{11/2})^3]_{16^-}$ configurations, respectively, and also at $I^{\pi}=19^{-}$, based on the $\pi[(g_{7/2})(h_{11/2})]_{9^-}\otimes\nu[(h_{11/2})^2]_{10^+}$ configuration. The 22^{+} state is only predicted for the heavier Te isotopes with $A\geqslant 118$; for the lighter isotopes, with a lower neutron Fermi surface, occupa-

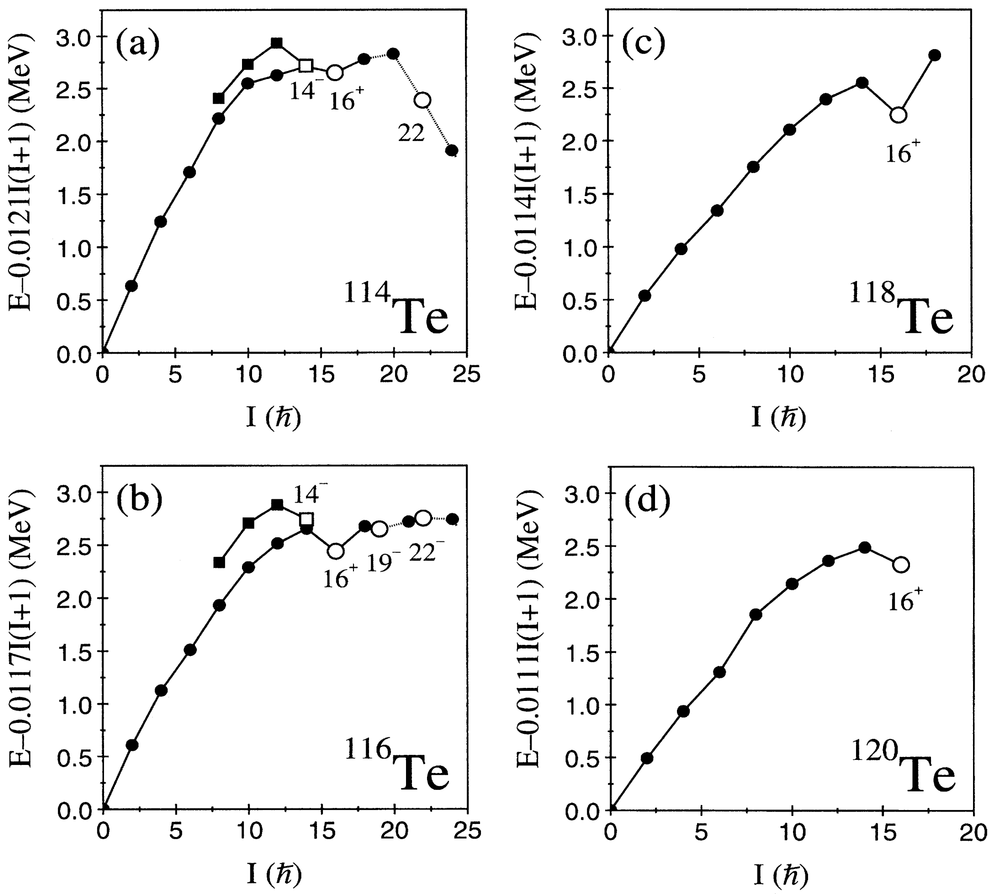

FIG. 2. Experimental rigid-rotor plots for ^{114}Te [18,25] (a), ^{116}Te [19,26] (b), ^{118}Te [20] (c), and ^{120}Te [21] (d). Dotted lines join states for which absolute spin and parity assignments are unknown. Possible aligned oblate states at $I^{\pi}=16^+$, 14^-, 19^-, and 22^- are denoted by the open symbols.

tion of four $h_{11/2}$ neutron orbitals is energetically expensive. Comparison of these predicted oblate states with experiment is difficult since absolute spin and parity assignments of the experimental states at high spin have not yet been determined; new data available from Gammasphere and Eurogam may help in this respect [25,26]. Evidence for the low-lying 19^- and 22^- oblate states does, however, exist for ^{116}Te [26], as shown in Fig. 2(b).

A theoretical rigid-rotor plot for ^{116}Te is presented in Fig. 3. The solid line represents positive-parity collective states with deformation parameters $\beta_2 \approx 0.15$ and $\gamma \approx 0°$; the ground-state band (GSB) is shown for $I \leqslant 10\hbar$, while at higher spin this band evolves into a collective $\nu[(h_{11/2})^2]$ two-quasiparticle configuration. The predicted oblate states are also shown in Fig. 3. It can be seen that the states at $I^{\pi}=16^+$, 19^-, and 22^- are yrast, or very near yrast. This theoretical diagram is to be compared with the experimental results of ^{116}Te shown in Fig. 2(b).

In the case of odd-A Te isotopes, unusually low-lying $39/2^-$ states have been observed in ^{117}Te [13] and ^{119}Te [14]. The TRS calculations [Fig. 1(b)] suggest a fully aligned $\pi[(g_{7/2})^2]_{6^+} \otimes \nu[(h_{11/2})^3]_{27/2^-}$ oblate configuration for these states. The experimental results for ^{119}Te are shown as a rigid-rotor plot in Fig. 4(a), where the $39/2^-$ state is clearly

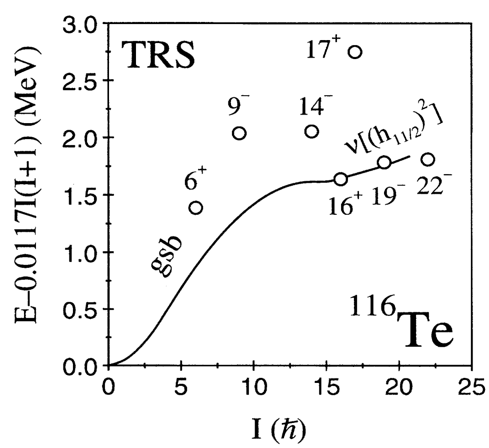

FIG. 3. Theoretical rigid-rotor plot for ^{116}Te obtained from the TRS calculations. The solid line connects weakly deformed prolate states, while several noncollective oblate states are denoted by open circles. Note the low-lying 16^+, 19^-, and 22^- states.

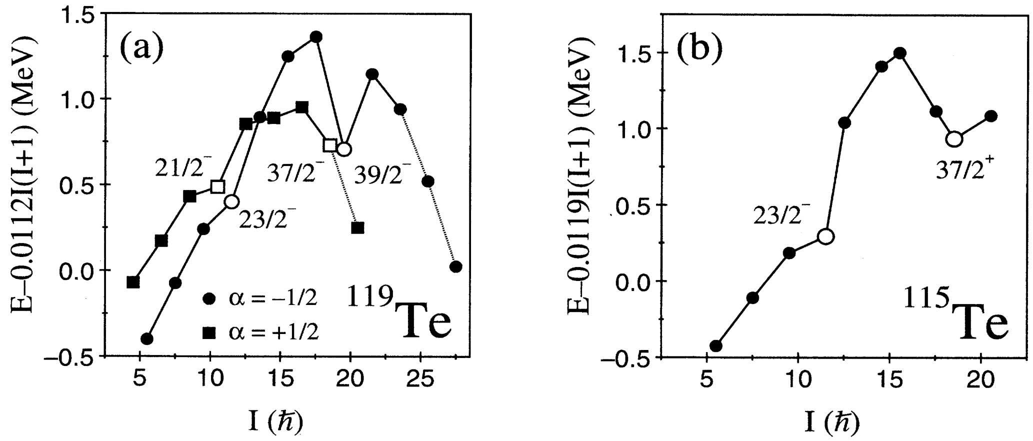

FIG. 4. Experimental rigid-rotor plots for ^{119}Te [14] (a) and ^{115}Te [27,26] (b). Dotted lines join states for which absolute spin and parity assignments are unknown. Possible aligned oblate states at $I^\pi = 21/2^-$, $23/2^-$, $37/2^-$, $39/2^-$, and $37/2^+$ are denoted by the open symbols.

seen to be favored with respect to the neighboring states. A low-lying oblate state at $I^\pi = 23/2^-$, based on the $\pi[(g_{7/2})^2]_{6^+} \otimes \nu[(h_{11/2})]_{11/2^-}$ configuration, is predicted for the $(-,-1/2)$ configuration. Indeed, there is a kink evident in Fig. 4(a) at this spin. States associated with the unfavored $(-,+1/2)$ configuration have also been established in ^{119}Te [14]. Theoretically, oblate states at $I^\pi = 21/2^-$ and $37/2^-$ are predicted for this signature. These states are closely related to the fully aligned $23/2^-$ and $39/2^-$ states and represent an $(I_{\max}-1)$ coupling of the aligned particles. The $I^\pi = 21/2^-$ and $37/2^-$ states are labeled in Fig. 4(a) for ^{119}Te.

The lighter ^{115}Te [27] isotope does not show a low-lying $39/2^-$ state. Instead, a change of parity is observed along the yrast line and a low-lying $37/2^+$ state is observed [27,26]. This is consistent with a noncollective oblate state predicted at $I^\pi = 37/2^+$ [Fig. 1(c)] based on the aligned $\pi[(g_{7/2})^2]_{6^+} \otimes \nu[(d_{5/2})(h_{11/2})^2]_{25/2^+}$ configuration. The disappearance of the $39/2^-$ state can be related to the low neutron Fermi surface in ^{115}Te, where the occupation of three $\nu h_{11/2}$ orbitals is energetically expensive. As in ^{117}Te [13] and ^{119}Te [Fig. 4(a)], a low-lying $23/2^-$ state is observed in ^{115}Te [Fig. 4(b)].

In summary, we have investigated theoretical predictions for noncollective oblate states in light Te isotopes, some of which compete energetically with the weakly deformed collective structures. Comparison with experimental data suggests that several of these oblate states have indeed been observed.

This work was in part supported by grants from the UK Engineering and Physical Science Research Council and the National Science Foundation. The authors are indebted to Dr. R. Wyss and Dr. W. Nazarewicz for providing the TRS cranking codes.

[1] I. Ragnarsson, Z. Xing, T. Bengtsson, and M.A. Riley, Phys. Scr. **34**, 651 (1986).
[2] W. Nazarewicz, J. Dudek, R. Bengtsson, and I. Ragnarsson, Nucl. Phys. **A435**, 397 (1985).
[3] S. Cwiok, J. Dudek, W. Nazarewicz, W. Skalski, and T. Werner, Comput. Phys. Commun. **46**, 379 (1987).
[4] R. Wyss, Ph.D. thesis, Manne Siegbahn Institute of Physics, Stockholm, 1990.
[5] S. Juutinen *et al.*, Z. Phys. A **338**, 365 (1991).
[6] J. Simpson, H. Timmers, M.A. Riley, T. Bengtsson, M.A. Bentley, F. Hanna, S.M. Mullins, J.F. Sharpey-Schafer, and R. Wyss, Phys. Lett. B **262**, 388 (1991).
[7] H. Timmers, J. Simpson, M.A. Riley, T. Bengtsson, M.A. Bentley, F. Hanna, S.M. Mullins, J.F. Sharpey-Schafer, and R. Wyss, J. Phys. G **20**, 287 (1994).
[8] J. Timár, J. Simpson, E.S. Paul, S. Araddad, C.W. Beausang, M.A. Bentley, M.J. Joyce, and J.F. Sharpey-Schafer, J. Phys. G **21**, 783 (1995).
[9] E.S. Paul *et al.*, J. Phys. G **18**, 837 (1992).
[10] M.P. Waring *et al.*, Phys. Rev. C **48**, 2629 (1993).
[11] Y. Liang, D.B. Fossan, J.R. Hughes, D.R. LaFosse, T. Lauritsen, R. Ma, E.S. Paul, M.P. Waring, P. Vaska, and N. Xu, Phys. Rev. C **45**, 1041 (1992).
[12] Y. Liang *et al.*, Phys. Rev. C **44**, R578 (1991).
[13] C. Duyar, J.E. Draper, E.C. Rubel, M.A. Deleplanque, R.M. Diamond, F.S. Stephens, E.M. Beck, and M.A. Stoyer, Z. Phys. A **348**, 63 (1994).
[14] J. Singh *et al.*, Z. Phys. A **351**, 3 (1995).
[15] W. Nazarewicz, G.A. Leander, and J. Dudek, Nucl. Phys. **A467**, 437 (1987).
[16] R. Wyss, J. Nyberg, A. Johnson, R. Bengtsson, and W. Nazarewicz, Phys. Lett. B **215**, 211 (1988).
[17] W. Nazarewicz, R. Wyss, and A. Johnson, Nucl. Phys. **A503**, 285 (1989).
[18] C.-B. Moon *et al.*, Phys. Rev. C **51**, 2222 (1995).
[19] A. Sharma, J. Goswamy, D. Mehta, J. Singh, H. Kaur, B.

Chand, N. Singh, R.K. Bhowmik, and P.N. Trehan, Z. Phys. A **346**, 321 (1993).

[20] A. Sharma, J. Singh, H. Kaur, J. Goswamy, D. Mehta, N. Singh, R.K. Bhowmik, and P.N. Trehan, Z. Phys. A **351**, 131 (1995).

[21] P. Chowdhury, W.F. Piel, Jr., and D.B. Fossan, Phys. Rev. C **25**, 813 (1982).

[22] E.S. Paul *et al.*, Phys. Rev. C **50**, 698 (1994).

[23] E.S. Paul, H.R. Andrews, V.P. Janzen, D.C. Radford, D. Ward, T.E. Drake, J. DeGraaf, and S. Pilotte, Phys. Rev. C **50**, R534 (1994).

[24] J. Simpson *et al.*, Phys. Lett. B **327**, 187 (1994).

[25] I. Thorslund *et al.*, Phys. Rev. C (submitted).

[26] J.M. Sears *et al.* (unpublished).

[27] C.-B. Moon *et al.*, Z. Phys. A **349**, 1 (1994).